Asphalt-rubber interaction and performance evaluation of rubberised asphalt binders containing non-foaming warm-mix additives

Wang, Haopeng; Liu, Xueyan; Zhang, Hong; Apostolidis, Panos; Scarpas, Tom; Erkens, Sandra

DOI
10.1080/14680629.2018.1561380

Publication date
2018

Document Version
Accepted author manuscript

Published in
Road Materials and Pavement Design

Asphalt-rubber Interaction and Performance Evaluation of Rubberized Asphalt Binders Containing non-foaming Warm-mix Additives

Haopeng Wang[a]*, Xueyan Liu[a], Hong Zhang[a], Panos Apostolidis[a], Tom Scarpas[a, b], and Sandra Erkens[a]

[a]*Section of Pavement Engineering, Faculty of Civil Engineering & Geosciences, Delft University of Technology, Stevinweg 1, 2628CN, Delft, The Netherlands;* [b]*Department of Civil Infrastructure and Environmental Engineering, Khalifa University, Abu Dhabi, United Arab Emirates*

*Corresponding author. Email: haopeng.wang@tudelft.nl

Xueyan Liu: x.liu@tudelft.nl

Hong Zhang: h.zhang-4@tudelft.nl

Panos Apostolidis: p.apostolidis@tudelft.nl

Tom Scarpas: a.scarpas@tudelft.nl

Sandra Erkens: s.m.j.g.erkens@tudelft.nl

Word count: 7545

Asphalt-rubber Interaction and Performance Evaluation of Rubberised Asphalt Binders Containing non-foaming Warm-mix Additives

Warm mix asphalt (WMA) technology has been increasingly utilised in rubberised asphalt pavements to reduce the production and compaction temperatures and the incidental fumes and odours. This study aims to investigate the high, intermediate and low-temperature performance of crumb rubber modified asphalt binders containing WMA additives. The asphalt-rubber interactions under various mixing combinations of temperature and time were investigated through both microscopic and mechanical methods to obtain the optimum mixing procedure. The effects of WMA additives (wax-based and chemical-based products) on the binder performance were investigated by multiple stress creep and recovery (MSCR) test, linear amplitude sweep (LAS) test and low-temperature frequency sweep test. Results show that rubberised asphalt binders significantly improve the binder performance of base asphalt at different temperature ranges. The effects of WMA additives on binder performance varied with base asphalt and rubberised asphalt binder. In addition, the nonrecoverable compliance difference was found not suitable to characterise the stress sensitivity of rubberised binders and the difference in the nonrecoverable compliance for an incremental change in applied stress was proved to be a more accurate alternative. For the cyclic LAS test, the failure energy was found to have a strong correlation with the predicted fatigue life using simplified viscoelastic continuum damage analysis and therefore can be considered as a simple indicator for binder fatigue performance ranking. Relaxation modulus and rate derived from low-temperature frequency sweep tests produced comparable results for ranking the low-temperature performance of different binders. It is feasible and promising to use a unified DSR test methodology to characterise the binder performance covering the whole service temperature range.

Keywords: crumb rubber modifier; warm mix asphalt; MSCR; LAS; frequency sweep

1 Introduction

According to the European Environment Agency report in 2015, the transport sector

contributed 25.8 % of the total European Union greenhouse gas (GHG) emissions (EEA, 2017). With the Paris climate agreement taking effect, the global transport sectors have been facing growing international pressure on the reduction of GHG emission and fossil fuel consumption. Meanwhile, with the transportation development and increasing number of vehicles on the roads, millions of end-of-life tires (ELTs) are produced every year. The rising environmental awareness has driven people to seek appropriate treatment and disposal of scrap tires, such as retreading, energy recovery and material recycling. In 2013, 96% of the waste tires (3.6 million tonnes) were recovered and recycled in the EU (ETRMA, 2016), which confirms the EU as a leading role in the waste management.

Among the transport infrastructure, the road construction is always a large consumer of energy and resource. In view of this, developing sustainable paving technologies with fewer consumptions of resource and energy as well as fewer emissions of GHG is a great concern for both transport agencies and the general public. The rubberised asphalt concrete technology has been applied in the asphalt paving industry for decades. It not only solves the disposal issues of scrap tires but also improves the overall performance of asphalt pavements with add-on value (Maupin Jr., 1996; Pasquini, Canestrari, Cardone, & Santagata, 2011; B. Yu, Jiao, Ni, & Yang, 2014). Warm mix asphalt (WMA) technology was developed to reduce the construction temperatures of asphalt pavements and thereby reduce the energy consumption and GHG emissions (D'Angelo, 2008; Hanz, 2012; National Asphalt Pavement Association, 2008). Combining WMA with rubberised asphalt technology not only reduces the production and compaction temperatures due to the high viscosity of rubberised asphalt binders but also provides better working conditions with reduced odours and fumes.

The individual effect of crumb rubber modifier (CRM) and various warm-mix additives on the binder properties has been extensively investigated (Lo Presti, 2013;

Rubio, Martínez, Baena, & Moreno, 2012). It was shown that the interactions of asphalt and rubber and their effects on the final properties of crumb rubber modified asphalt (CRMA) depend on the raw material parameters (e.g., asphalt composition, CRM type, morphology, particle size and dosage) and interaction conditions (e.g., mixing temperature, time and rate, energy type of the mechanical mixing exerted) (M. Abdelrahman, 2006; Airey, Rahman, & Collop, 2011; Shen & Amirkhanian, 2007). The two main interaction mechanisms involved in the production of CRMA binders are rubber particle swelling and chemical degradation (devulcanization and/or depolymerization) in the binder matrix (M. A. Abdelrahman & Carpenter, 1999). The incorporation of CRM into asphalt binders was reported to improve the overall pavement performance, e.g., higher resistance to rutting, ageing, fatigue and thermal cracking (Shu & Huang, 2014). It also increases the skid resistance of pavements and reduces the traffic noise (Rymer & Donavan, 2005), which provides a safe and comfortable driving condition. More importantly, it was proved that rubberized asphalt pavement can be recycled using conventional equipment and practices with minor modifications (California DOT, 2005). The effect of WMA technology on the performance of asphaltic materials varies with the type of WMA technology used (Rubio et al., 2012). However, the influence of WMA additives on the crumb rubber modified asphalt binders has not yet been clearly identified. The interactions between asphalt and rubber, as well as the WMA additives, have a significant impact on the mechanical performance and durability of warm-mix rubberised asphalt pavements (Ragab & Abdelrahman, 2014). Because of the complicated relationship between the individual components of warm-mix rubberised asphalt mixture, it is essential to understand their interactions in the rubberised binders before applying them to the mix design level. With an optimised material design and reliable performance evaluations, warm-mix rubberised asphalt is believed to be a sustainable paving

technology with tremendous economic, environmental and social benefits (Wang, Liu, Apostolidis, & Scarpas, 2018b).

2 New-generation performance-related testing of binders

Permanent deformation, fatigue cracking and thermal cracking are three primary forms of distress which are highly correlated to high, intermediate and low-temperature range in asphalt pavements. Extensive research has shown that the mechanical characteristics of asphalt binder-mastic phase has predominant effects on the final performance of asphalt mixture (Bahia et al., 2001). Current performance related binder specifications were primarily developed for unmodified binders and were based on linear viscoelastic properties of the material. For example, the rutting resistance of asphalt binders in Superpave is determined based on limiting criteria on the minimum parameter ($|G^*|/\sin\delta$) value obtained at high temperatures. The fatigue resistance of asphalt binders is addressed by placing a maximum limit on the parameter ($|G^*|\cdot\sin\delta$) at intermediate temperatures. However, it has been proven that the two complex modulus-phase angle based parameters of asphalt binders obtained by Dynamic Shear Rheometer (DSR) have poor correlations with the mixture/pavement performance, especially for modified binders which often demonstrate superior damage resistance (Bahia et al., 2001). Therefore, a number of new testing methods have been proposed in recent years for damage characterisation of asphalt binders considering non-linear viscoelasticity. Among them, multiple stress creep and recovery (MSCR) test and linear amplitude sweep (LAS) test of asphalt binders were found to be more successful in correlating with mixture performance and have been proposed to provide efficient test and analysis methods for measuring the high-temperature rutting resistance and intermediate-temperature fatigue resistance, respectively (D'Angelo & Dongré, 2009; Hintz & Bahia, 2013; Hintz, Velasquez, Johnson, & Bahia, 2011; Masad, Huang, DAngelo, & Little, 2009). In terms

of the low-temperature performance test, a recently developed 4-mm DSR employing 4-mm diameter parallel plates was proposed as an alternative with a number of advantages to the bending beam rheometer (BBR) (FHWA, 2017). Therefore, in principle, asphalt binder properties in the whole temperature range can be characterised by using only one DSR instrument with different accessories (4, 8- and 25-mm diameter plates). The choice of the parallel plate size is generally dependent on the testing temperatures. This unified DSR method is believed to be a technical breakthrough allowing improvement in the ability to provide performance-related specifications for road paving materials.

3 Objectives

Based on aforementioned considerations, the main objectives of this study are:

- to investigate the asphalt-rubber interaction and determine the optimum mixing parameters of CRMA binders for given materials, and
- to investigate the effects of WMA additives on the high-temperature, fatigue and low-temperature performance of base asphalt and rubberised asphalt binders using new-generation test methods.

4 Materials and methods

4.1 Materials

For clarification, "asphalt" in this paper represents the binder instead of the mix. Base asphalt of 70/100 penetration grade commonly used in the Netherlands was provided by NYNAS. The SARA fractions of the base asphalt are 7% for saturates, 51% for aromatics, 22% for resins, and 20% for asphaltenes, respectively. The ambient grinding CRM has particle sizes ranging from 0 to 0.5 mm. The basic properties and composition of CRM are shown in Table 1. The morphology of CRM used in this study was obtained through Environment Scanning Electron Microscopy (ESEM) in Fig. 1a. The ESEM images

confirmed that rubber particles from ambient grinding have an irregular shape and fluffy appearance with higher surface area than the cryogenic ones. It was reported that large surface area will promote the interaction of asphalt and rubber, causing the faster absorption of lightweight components from asphalt into rubber, which will enhance the properties of the final binders (Shen & Amirkhanian, 2007). This study included two types of non-foaming WMA additives, wax-based product **W** and chemical-based product **C**. Additive W is a synthetic microcrystalline wax that is free of sulfur and other impurities. Additive C is a liquid chemical package of products, such as surfactants, polymers, additives, anti-stripping agents, etc.

4.2 Sample preparation for ESEM tests

To have a visualised observation on the interaction between asphalt and rubber, ESEM with energy dispersive X-ray spectroscopy (EDX) was utilised to investigate the morphology and element composition of both asphalt and rubber as well as their blends. Based on trial tests, it is difficult to see the morphological difference between different CRMA binders produced at different interaction conditions when using the fine CRM particles in this study. This is because the observation results were highly dependent on the binder samples scooped from the batch. It is impossible to guarantee the uniform sized rubber particles in the binder matrix between different samples. Therefore, an alternative way was used to investigate the effects of temperature and time on the asphalt-rubber interaction. A type of heat-casting method developed by Mikhailenko et al. (Mikhailenko, Kadhim, & Baaj, 2017) was adopted to prepare the samples for ESEM test. The base asphalt stored in the container was first heated at 110 °C for approximately 1 h for later use. Approximately 0.1 g asphalt was extracted from the container into the cylindrical sample holder (9.5 mm in diameter and 5.2 mm in height) with a spatula. The sample holder was then placed on a heater at 150 °C for about 10 s to flatten the sample. To

prepare the asphalt rubber blends for interaction, a small amount of CRM particles was carefully spread on the surface of the asphalt on the holder at 110 °C. This state was assumed as the reference state where no substantial interactions between asphalt and rubber happened. All the prepared samples were then stored in a covered plastic container in the refrigerator at around 0 °C overnight before the ESEM tests (Fig. 2).

After obtaining the SEM images and EDX spectrums of asphalt-rubber blend samples at the reference state, these samples were heated at 160, 180, 200 °C for 30 min respectively. Then the interacted samples were subjected to the ESEM analysis again.

4.3 Sample preparation for DSR tests

For given base asphalt and CRM, the interactions of asphalt and rubber are functions of mixing temperatures, time and rate. Since the mixing rate has a similar effect as the mixing time (A. Ghavibazoo, Abdelrahman, & Ragab, 2013), only two interaction variables (temperature and time) were considered in this study to determine the optimised mixing procedure to produce desirable CRMA binders. The dosage of CRM was set as 18% by the weight of the total blend based on previous studies (Huang, 2008; Wang, Liu, Apostolidis, & Scarpas, 2018a). Manual stirring for 5 min was applied to pre-distribute CRM in the base asphalt, then the blend was mixed using a Silverson high shear mixer (Fig. 3) at 6000 rpm with different combinations of temperature and time. Three interaction temperature levels were chosen: 160 °C, 180 °C, and 200 °C. At each temperature, different mixing time, 30 min, 60 min, 90 min were applied for the CRMA blends.

After preparing the CRMA binders using optimised mixing procedure, each WMA additive was blended with both base binder and CRMA binder at 140 °C. It should be mentioned that WMA additives did not participate the interaction of asphalt and CRM at high temperatures. The percentages of wax-based W and chemical-based C were 2.0%

and 0.6% for both base asphalt and CRMA binders, which were determined based on manufacturers' recommended dosage and preliminary tests. Therefore, a total of six types of asphalt binders were prepared for performance characterisation, namely 70/100, 70/100-W, 70/100-C, CRMA, CRMA-W, and CRMA-C. To solely investigate the effect of WMA additives on the rheological properties of binders, all binder samples were tested in a fresh state without the artificial ageing procedure.

4.4 Testing Methods

4.4.1 ESEM Test with EDX

The observations for all the samples were conducted using a Philips XL30 ESEM with an EDX (Fig. 4). The equipment setting parameters were as follows: an acceleration voltage of 20 keV, a spot size (size of the electron probe) of 5.0 nm, a chamber pressure of 1 Torr and temperature of 0 °C in low vacuum mode, and magnification of 100× using a backscattered electron detector (BSD). The electron gun was kept at a distance of 10 mm from the surface of the sample. After obtaining the SEM images, elemental analysis is accomplished at selected spots using an energy dispersive X-ray spectroscopy detector. The EDX system can detect the chemical composition of the materials and create elemental composition maps based on the collected energy spectra (Divya, Gideon, & Krishnan, 2013).

4.4.2 Multiple Stress Creep and Recovery Test

The MSCR test was conducted using a DSR at two stress levels (0.1 kPa and 3.2 kPa) at 64 °C according to AASHTO T350-14. The test protocol includes a creep load of 1 s duration followed by 9 s recovery at zero loads in each cycle. Ten creep and recovery cycles were tested at each stress level. The nonrecoverable creep compliance (J_{nr}) and

the percentage of recovery were calculated to characterise the stress dependence and elastic response of asphalt binders.

4.4.3 Linear Amplitude Sweep Test

The LAS test has recently been proposed for accelerated fatigue characterisation of asphalt binders (AASHTO TP 101-14). The LAS test consists of cyclic loading employing systematically, linearly increasing strain amplitudes. The amplitude sweep is conducted using the DSR with the standard 8-mm parallel plate geometry at the frequency of 10 Hz. The strain is increased linearly from 0.1 to 30% over the course of 3,100 cycles of loading to induce fatigue damage at an accelerated rate. Before the LAS test, a frequency sweep test is also performed on the same specimen to obtain the undamaged linear viscoelastic properties of materials. The frequency sweep test employs a constant load of 0.1% strain over a range of frequencies from 0.2 to 30 Hz. The LAS test temperature was chosen as 25 °C. Simplified viscoelastic continuum damage (S-VECD) modelling can be applied to the LAS test results to quantify the damage and predict the fatigue life at any strain amplitude of interest (Hintz et al., 2011).

4.4.4 Frequency Sweep Test at Low Temperatures

The newly developed 4-mm DSR, referring to performing frequency sweep tests with 4-mm diameter parallel plates, can reliably determine the low-temperature linear viscoelastic properties to provide a performance-related binder specification test method. The general concept of this technique is to establish a correlation between bending beam rheometer (BBR) creep stiffness and the shear relaxation modulus from DSR as well as between their corresponding apparent relaxation rates (Farrar, Sui, Salmans, & Qin, 2015; Sui, Farrar, Harnsberger, Tuminello, & Turner, 2011). Considering the climate conditions in the Netherlands, the frequency sweep tests were performed from 0.1 to 100 rad/s at

different low temperatures (-10, 0 and 10 °C) with updated DSR from Anton Paar which can make the real-time online instrument compliance correction. Before the frequency sweep tests, strain amplitude sweep tests were conducted to identify the linear viscoelastic (LVE) range of different binders and thus to ensure the frequency sweep tests were undertaken within the binder's LVE region of response. Based on the LVE limits, all the measurements were carried out at a strain level of 0.1% under strain-controlled mode. Then, master curves at a reference temperature of -10 °C are constructed for later low-temperature parameter analysis.

5 Results and discussions

5.1 ESEM Investigation of Morphology and Elemental Composition

The morphology and elemental composition of CRM was analysed by the ESEM images and EDX spectra (Fig. 5). The EDX spectrum was presented as a plot of X-ray counts versus energy (keV). The energy peaks corresponding to the various elements in the sample are also shown. It should be noted that elements lighter than the atomic number of Na cannot be detected. The asphalt surface is very homogenous except some impurities and contains primarily the elements of C and S. In contrast, CRM contains a variety of chemical compounds (e.g., zinc, iron and silicon, etc.) which base asphalt does not possess.

To investigate the asphalt-rubber interactions at different temperatures, the ESEM images of the samples at different interaction conditions were shown in Fig. 6. In Fig. 6a, the edge of rubber particles is sharp and clearly to define at the reference state. In Fig. 6b, the interface between asphalt and rubber became vague after 30 min interaction at 160 °C illustrated by the white ellipse. Swelling of rubber to a certain extent was also observed. With the increase of interaction temperature to 180 °C (Fig.6c), more and more rubber

particles dissolved into the asphalt matrix. At 200 °C, it was difficult to find the rubber particle islands and to define the interface between asphalt and rubber. This clearly showed that high temperature can promote the digestion of CRM into asphalt. Elemental analysis was also carried out on the reacted samples. It can be seen from Fig. 7 that some new elements (e.g., Zn, Cu, Si) coming from CRM showed up in the asphalt matrix after interaction at 160 °C for 30 min. In addition, the counts of element C in the interacted asphalt matrix increased compared to the base asphalt. This confirmed that component exchange between asphalt and rubber took place during the interaction. Results at other temperatures also showed similar findings. Visualised observations can offer direct information about the interaction However, the mechanical properties of rubberised asphalt binders are still unknown yet, which needs property characterisation to have a further understanding of the interaction.

5.2 Optimizing the Asphalt-Rubber Interaction Procedure

From the results of previous MSCR tests with various modified asphalt binders, it was known that MSCR test method is sensitive to the microstructure of the polymer modified binders (D'Angelo & Dongré, 2009). It is anticipated that MSCR test can be also utilised to characterise the microstructural changes of CRMA binders at various interaction conditions. In this study, test samples for MSCR were prepared and moulded immediately after the interactions to avoid reheating the solidified CRMA binders, which may cause potential interactions within the binders and therefore produce confounded results. Three replicates were prepared for each sample.

Fig. 8 shows a typical plot of creep and recovery cycle at 3.2 kPa. For brevity, only the results of CRMA binders prepared with 30-min mixing were shown. The effects of interaction on the creep and recovery behaviours of CRMA binders are clearly identified by the distinct stress-strain responses. The reason for the different responses

were explained followingly. Specifically, the MSCR J_{nr} values and percentages of recovery of CRMA binders with different interaction combinations at 3.2 kPa are illustrated in Fig. 9. In general, both J_{nr} and percentage of recovery show different trends with the increasing interaction temperatures, which implies that there may be different interaction mechanisms happened during the mixing process. At a relatively low temperature of 160 °C, swelling of rubber particles continuously happened over the entire interaction period as illustrated by the continual decrease in compliance value. Rubber particles were swollen by absorption of the aromatic oils from asphalt matrix to form a gel-like structure. The change in rubber particle volumes and formation of gel structures in the binder reduces the distance between swollen rubber particles, and therefore stiffening the composite material. At the intermediate temperature of 180 °C, both J_{nr} and recovery only had limited changes. The flat curves showed the CRMA binder interacted at 180 °C reached a certain equilibrium. Based on the previous research (M. Abdelrahman, 2006), it was known that at this temperature level, swelling happened faster than at 160 °C. Since CRMA binders prepared at 180 °C for 30 min exhibited similar J_{nr} as the one prepared at 160 °C for 90 min, it is possible that swelling reached the same level at 180 °C for 30 min as at 160 °C for 90 min. After 30-min interaction at 180 °C, a small amount of the swollen rubber particles started depolymerization, releasing some polymeric components to the asphalt matrix. Although the J_{nr} slightly increased, the percentage of recovery also slightly increased, indicating the binder became more elastic. At the high temperature of 200 °C, rubber particles reached the swelling equilibrium in a very short time (Artamendi & Khalid, 2006). Generally, swelling of elastomeric polymers (rubber) in organic solvents (aromatic oils) is a diffusion process (Buckley & Berger, 1962). As the temperature increases, the diffusion coefficient also increases, which accelerates the swelling process. Noticing from Table 1 that the

decomposition temperature of CRM is around 200 °C, the significant increase of J_{nr} and decrease of percentage of recovery at 200 °C were mainly due to the depolymerization and/or devulcanization of rubber particles. The degradation of rubber particles at high temperature destructed the polymer network and cross-linking structure, resulting in a less elastic response. In addition, the potential binder ageing at such a high temperature may also leaded to the increase of of J_{nr} and decrease of percentage of recovery.

The above analysis clearly shows the dominant effect of temperature on the swelling and degradation process of rubber particles. Fig. 10 illustrates the different stages of asphalt-rubber interactions with increasing interaction temperatures and time. Initially, at low temperatures, swelling of rubber particles continuously happens at a low speed to form a gel-like material (Stage 1). With the increase of temperature, rubber particles swell fast and reach the swelling equilibrium quickly (Stage 2). At this stage, only limited degradation of rubber particles happens. When the temperature reaches a certain elevated level, degradation of swollen rubber particles happens drastically (Stage 3). The observations here correlated well with the ESEM investigation.

Based on above analysis, mixing asphalt and rubber at 180 °C for 30 min was chosen as the optimised asphalt-rubber interaction procedure, which produces CRMA binders with lower J_{nr} and higher percentage of recovery. In addition, from a practical viewpoint, the asphalt-rubber interaction is more stable at 180 °C with the increase of interaction time, which makes it easy for CRMA product quality assurance/control in plants.

5.3 High-temperature Performance of Asphalt Binders

Table 2 summarises the MSCR test results of both base asphalt and CRMA with WMA additives. The CRMA binder prepared at the proposed procedure had a much lower J_{nr}

and a higher percentage of recovery at 3.2 kPa than the base asphalt, indicating a superior polymer network established by the asphalt-rubber interaction. The addition of a wax-based additive to base asphalt decreased J_{nr} value, but did not significantly change the percent recovery at 3.2 kPa. The improvement of resistance to permanent deformation stems from the microcrystalline structure of W at the temperature below its melting point. The lattice structure formed by uniformly distributed wax particles at service temperature stiffens the binder. The chemical-based additive seemed to make the base binder a bit softer and slightly increased the percent recovery. Different effects of warm-mix additives on the MSCR results of CRMA binders were observed as shown in Table 2. This difference is possibly due to the potential physical or chemical interactions between asphalt, rubber and warm-mix additives which needs further research.

The J_{nrdiff} parameter, defined as the difference of J_{nr} at different stress levels, is intended to evaluate the stress sensitivity of binders and is imposed an upper limit of 75%. It can be seen from Table 2 that all CRMA binders and W modified base asphalt exceeded the maximum allowable J_{nrdiff} value. However, the low J_{nr} values of these binders prove adequate resistance to permanent deformation at high service temperatures. It seems the J_{nrdiff} parameter lacks universality to characterise the stress sensitivity of highly modified binders. Other research also confirmed this statement and recommended not evaluating the J_{nrdiff} parameter for accreditation purposes (Malusky, 2016). In this context, an alternate parameter $J_{nrslope}$ defined as the change in J_{nr} for an incremental change in applied stress τ, was proposed (Stempihar, Gundla, & Underwood, 2018).

$$J_{nrslope} = \frac{dJ_{nr}}{d\tau} = \frac{J_{nr3.2} - J_{nr0.1}}{\tau_{3.2} - \tau_{0.1}} \times 100 \quad (1)$$

From Table 2, it can be seen all binders except for 70/100-W meet the requirement of

stress sensitivity using the $J_{nrslope}$ parameter, which can be considered a more accurate assessment of stress sensitivity. In addition, CRMA based binders exhibited superior stress insensitivity as expected using the new parameter.

5.4 Fatigue Performance of Asphalt Binders

5.4.1 Simplified Viscoelastic Continuum Damage Modelling of LAS Results

S-VECD modelling of asphalt binders is based on Schapery's work potential theory that utilises an internal state variable to represent damage (*D*) because of microstructural changes that lead to the loss of material integrity (*C*). The relationship between damage and material integrity at any time (*t*) can be derived from the work potential theory and calculated with Equation 2.

$$D(t) \cong \sum_{i=1}^{N} [\pi {\gamma_0}^2 (C_{i-1} - C_i)]^{\frac{\alpha}{\alpha+1}} (t_i - t_{i-1})^{\frac{1}{1+\alpha}} \quad (2)$$

where $C(t) = |G^*(t)|/|G^*_{initial}|$, material integrity; γ_0 = applied strain for a given cycle (%); $G^*(t)$ = complex shear modulus at time *t* (MPa); $G^*_{initial}$ = the initial undamaged complex shear modulus (MPa); α = parameter determined from frequency sweep test data; *i* = time step; *N*=total time steps.

To incorporate the S-VECD model into fatigue life prediction, a power law model is developed to fit the material integrity versus damage curve according to Equation 3.

$$C(t) = 1 - C_1 (D)^{C_2} \quad (3)$$

where C_1 and C_2 = coefficients derived from the curve-fitting. The fatigue failure point is defined as the peak shear stress which corresponds the marked change in the loss of material integrity. The damage value at failure (D_f) is further calculated as given in Equation 4.

$$D_f = \left(\frac{1 - C_{peak\ stress}}{C_1}\right)^{1/C_2} \quad (4)$$

Finally, the fatigue law describing the relationship between fatigue life (N_f) and the strain amplitude (γ_{max}) can be expressed as

$$N_f = A(\gamma_{max})^{-B} \quad (5)$$

where A = fatigue model parameter defined as Equation 6; $B = -2\alpha$.

$$A = \frac{f(D_f)^k}{k(\pi C_1 C_2)^\alpha} \quad (6)$$

where $k = 1 + (1 - C_1)\alpha$; f = loading frequency (Hz).

5.4.2 Analysis of LAS Results

During the DSR measuring of test samples, the apparent shear stress at the sample edge is monitored and reported. However, this apparent edge stress is calculated using a linear radial mapping to the total torque, which is erroneous in the presence of material or geometric nonlinearity such as cracking. Therefore, the shear stress and strain mentioned here are apparent shear stress and strain when the LAS analysis is performed. Although the effect of nonlinearity is neglected for simplicity in LAS test, rankings of predicted fatigue life from LAS analysis remained in good agreement with measured fatigue lives in time sweep tests (Safaei & Castorena, 2016). Therefore, the current LAS analysis protocol is still used in this study for practical and efficient fatigue characterisation of asphalt binders.

Fig. 11 presents the plot of apparent shear stress versus strain from the LAS test results. At the very initial stage, with the increase of strain amplitude, the shear stress increased proportionally. With the continuous increase of strain amplitude, the increasing rate of shear stress slowed down where asphalt binders entered the nonlinear regions. When the strain increased to certain values depending on the type of asphalt binder, the

peak shear stress came up. After that, the shear stress continuously decreases with the increase of loading strain, indicating severe damage induced in the material. Comparing base asphalt with CRMA, when the base asphalt reached the stress peak and started to decrease, the shear stress of CRMA was still increasing. This indicated that CRMA was still integrated enough to sustain this strain level, which can be attributed to the higher damage resistance of CRMA. The addition of warm mix additives to the binder did not significantly change the behaviours of the binders under shear loading.

The different stress-strain responses of asphalt binders were further analysed using S-VECD modelling. The measured *C* versus *D* damage characteristic curves of various binders are shown in Fig. 12. It is clear that materials showed different damage evolution characteristics because of the different damage resistance. To allow for the fatigue performance prediction, the damage characteristic curves were fitted using Equation 3 to obtain the model parameters. For brevity, only the comparison between experimental data and model fitting of CRMA binder without additives is shown in Fig. 12c. From the fitted model curves, the integrity parameter of asphalt binder can be obtained at any particular damage intensity, indicating the material's ability to resist damage. An integrated S-VECD fatigue characterisation consists of three material function parts, linear viscoelastic property, damage characteristic curve, and fatigue failure criterion. With the analysis of these three functions, the S-VECD model parameters are summarised in Table 3 to identify the fatigue performance. The fatigue performance of asphalt pavements is a function of both material's damage resistance and loading strain amplitude. The predicted fatigue lives corresponding to two binder strain levels (different asphalt layer stiffness) using Equation 5 are also presented in Table 3. In addition, the failure energy defined as the area under stress-strain curve up to the failure point were calculated and summarised in Table 3.

From Table 3, it can be found that there is an enormous difference between the predicted fatigue lives of base asphalt and CRMA. The dramatic increase in fatigue life of CRMA can be attributed to the polymer network formed in CRMA binder. The effects of WMA additives on the fatigue performance of CRMA binder are different from base asphalt. Both wax-based and chemical-based WMA additives slightly increased the fatigue life of base asphalt. However, both WMA additives showed adverse effects on the fatigue performance of CRMA binder. The different effects of WMA additives on the fatigue performance coincides with the results of MSCR tests. This difference is possibly due to the more complex interactions between asphalt and WMA additives influenced by the addition of CRM, which was also reported by others (H. Yu, Leng, Xiao, & Gao, 2016). The added WMA additives had influence on the interaction between asphalt and CRM which needs further research. In Fig. 13, a strong correlation is found between the predicted fatigue life at the binder strain level of 2.5% from S-VECD model and failure energy, indicating that failure energy is an effective parameter for ranking the binder fatigue resistance without rigorous S-VECD analysis. However, this statement relies on the definition of fatigue failure criterion. More LAS test results of various binders can be obtained to further verify this finding.

5.5 Low-temperature Performance of Asphalt Binders

5.5.1 Determination of shear stress relaxation modulus and relaxation rate

Low-temperature rheological parameters such as BBR *m*-value and creep stiffness $S(t)$ can be estimated through a correlation with DSR data. The slope and magnitude of the shear stress relaxation modulus $G(t)$ master curve at 60 s are correlated with the corresponding creep stiffness $S(t)$ and *m*-values at 60 s from BBR measurement at the same low temperature. Based on the standard method proposed by Western Research

Institute (WRI) (FHWA, 2017), the main steps to determine the shear relaxation modulus and relaxation rate at 60 s, $G(60\text{ s})$ and $m_r(60\text{ s})$ from the DSR data include:

(1) Generate a storage modulus master curve at a reference temperature using the frequency sweep data;

(2) Determine relaxation modulus $G(t)$ through interconversion of the storage modulus $G'(\omega)$ by the approximate expression in Equation 7;

$$G(t) \approx G'(\omega)|\omega = 2/\pi t \quad (7)$$

(3) Determine the value of $G(60\text{ s})$ and $m_r(60\text{ s})$ through the relaxation modulus master curve by taking the first derivative.

The dynamic data were fitted with the Christensen-Anderson-Marasteanu (CAM) model. Through interconversion using Equation 7, the shear relaxation modulus master curves of different binders at a reference temperature of -10 °C were shown in Fig. 14. The relaxation modulus curve was fitted with a 2nd order polynomial for later calculation of $G(60\text{ s})$ and $m_r(60\text{ s})$. The resulting 2nd order polynomial and calculated $G(60\text{ s})$ and $m_r(60\text{ s})$ were summarised in Table 4.

5.5.2 Analysis of low-temperature performance

According to the experimental work performed at WRI, a simple linear correlation was derived between the BBR parameters ($S(60\ s)$ and $m_c(60\text{ s})$) and the DSR parameters ($G(60\ s)$ and $m_r(60\text{ s})$). The proposed limiting criteria (Farrar et al., 2015) were as follows: $G(60\ s)$<143 MPa at PG+10 °C corresponding to $S(60\ s)$<300 MPa; $m_r(60\text{ s})$>0.28 at PG+10 °C corresponding to $m_c(60\text{ s})$>0.30. Although there is some doubt about equivalency between the results obtained from BBR and DSR because of the

different cooling media and subsequent thermal history subjected to the specimen prior to testing (Marasteanu & Cannone Falchetto, 2018), the philosophy proposed here is still quite useful to rank the low-temperature performance of different binders. Fig.16 summarised the derived values of $G(60\ s)$ and $m_r(60\ \text{s})$ of different binders at -10 °C from Table 4. Generally, binders with lower stiffness and higher relaxation rate have better resistance to low-temperature cracking. The addition of wax-based additive stiffened the base asphalt, which increases the stiffness and decreases the relaxation rate. This is possibly due to the crystallization of wax in the binders at low temperatures which has a stiffening effect. In contrast, the addition of chemical WMA additive made the base asphalt softer by decreasing its stiffness and increasing the relaxation rate. Similar effects of chemical WMA additive were found on the crumb rubber modified asphalt while wax-base additive slightly changed the stiffness and relaxation rate of CRMA. In short, the wax-based additive has contradictory effects on base asphalt and CRMA while chemical additive improved the low-temperature cracking performance. The polymers and anti-stripping agents in the chemical additive are responsible for the improvement of cracking resistance. However, the conclusion needs to be further verified on the long-term aged samples. Comparing the base asphalt and CRMA, the addition of CRM can decrease the stiffness of the asphalt at low temperatures because of the presence of elastic CRM particles in the asphalt matrix. The elastic behaviour of CRMA was also demonstrated in the master curve of phase angle (Wang, Liu, Apostolidis, & Scarpas, 2018c). However, the relaxation rate was lowered indicating deteriorated flow capacity of asphalt. This can be explained by that the aromatic and light molecular weight fractions of asphalt were absorbed by CRM particles which eventually influence the relaxation rate (Amir Ghavibazoo & Abdelrahman, 2014). The above findings are consistent with previous studies using BBR tests to characterise the low-temperature performance of binders

(Akisetty, Lee, & Amirkhanian, 2010).

6 Conclusions and recommendations

This research investigated the asphalt-rubber interaction at various mixing combinations of temperature and time. The effect of two WMA additives on the high, intermediate and low-temperature performance of base asphalt and CRMA binder were also examined using MSCR, LAS and low-temperature frequency sweep tests. Based on the laboratory test results, the following conclusions can be drawn:

- The asphalt-rubber interaction is highly mixing temperature and time-dependent. With the increase of interaction temperature, the swelling and degradation of rubber particles successively occurred. The optimum asphalt-rubber interaction condition was determined at the mixing temperature of 180 °C for 30 min, which produced CRMA binders with lower nonrecoverable compliance and a higher percentage of recovery based on MSCR tests.

- The J_{nrdiff} parameter is not suitable to characterise the stress sensitivity of highly rubber modified binders. An alternate parameter defined as the change in J_{nr} divided by the increment of applied stress is a more accurate indicator of stress sensitivity.

- CRMA binders showed superior high-temperature performance and fatigue performance than base asphalts due to the rubber modification. CRMA also decrease the stiffness of asphalt at low temperatures which is advantageous.

- The effects of WMA additives on the rutting, fatigue and low-temperature cracking resistance of base asphalts are different from that of CRMA binders. Wax-based additive improved the high-temperature performance and fatigue

performance of base asphalt but deteriorated the low-temperature performance. Chemical-based additive slightly decreased the rutting resistance and improved the fatigue performance and thermal cracking resistance of base asphalt. In contrast, both WMA additives had adverse effects on the rutting and fatigue resistance of CRMA binders but had different effects on the low-temperature performance.

- The failure energy defined as the area under the stress-strain curve of LAS tests up to the failure point has a strong correlation with the predicted fatigue life of binders from the rigorous S-VECD analysis. Therefore, the LAS test-based failure energy can be considered as a simple and reliable indicator for ranking the fatigue performance of different binders.

- Through this preliminary study, it is feasible and promising to use a unified DSR test methodology to characterise the binder performance covering the whole service temperature range.

The ageing properties of rubberised asphalt binder with WMA additives should be investigated. More verification tests at both binder level and mixture level need to be done to establish a unified DSR test methodology for binder performance testing.

Acknowledgement

The authors acknowledge RUMAL for providing testing materials. The corresponding author would like to thank the financial support from China Scholarship Council. Special thanks are given to Arjan Thijssen from Microlab at Delft University of Technology for his guidance on performing ESEM tests.

Declarations of interest: none.

References

Abdelrahman, M. (2006). Controlling performance of crumb rubber-modified binders through addition of polymer modifiers. *Transportation Research Record: Journal of the Transportation Research Board*(1962), 64-70

Abdelrahman, M. A., & Carpenter, S. H. (1999). Mechanism of the interaction of asphalt cement with crumb rubber modifier. *Transportation Research Record: Journal of the Transportation Research Board, 1661*, 106-113

Airey, G., Rahman, M., & Collop, A. C. (2011). Crumb Rubber and Bitumen Interaction as a Function of Crude Source and Bitumen Viscosity. *Road Materials and Pavement Design, 5*(4), 453-475. doi: 10.1080/14680629.2004.9689981

Akisetty, C. K., Lee, S. J., & Amirkhanian, S. N. (2010). Laboratory investigation of the influence of warm asphalt additives on long-term performance properties of CRM binders. *International Journal of Pavement Engineering, 11*(2), 153-160. doi: 10.1080/10298430903197225

Artamendi, I., & Khalid, H. A. (2006). Diffusion kinetics of bitumen into waste tyre rubber. *Journal of the Association of Asphalt Paving Technologists, 75*, 133-164

Bahia, H. U., Hanson, D. I., Zeng, M., Zhai, H., Khatri, M. A., & Anderson, R. M. (2001). *Characterization of Modified Asphalt Binders in Superpave Mix Design*. Washington D.C. Retrieved from NCHRP Report 459.

Buckley, D. J., & Berger, M. (1962). The swelling of polymer systems in solvents. II. Mathematics of diffusion. *Journal of Polymer Science, 56*(163), 175-188

California DOT. (2005). *Feasibility Of Recycling Rubber-Modified Paving Materials*. California, USA.

D'Angelo, J., & Dongré, R. (2009). Practical Use of Multiple Stress Creep and Recovery Test. *Transportation Research Record: Journal of the Transportation Research Board, 2126*, 73-82. doi: 10.3141/2126-09

D'Angelo, J. (2008). *Warm-mix asphalt: European Practice*. Washington, DC.

Divya, P. S., Gideon, C. S., & Krishnan, J. M. (2013). Influence of the Type of Binder and Crumb Rubber on the Creep and Recovery of Crumb Rubber Modified Bitumen. *Journal of Materials in Civil Engineering, 25*(4), 438-449. doi: 10.1061/(Asce)Mt.1943-5533.0000608

EEA. (2017). *Greenhouse gas emissions from transport*. Denmark: European Environment Agency.

ETRMA. (2016). *End-of-life Tyre Report 2015*. Brussels.

Farrar, M., Sui, C., Salmans, S., & Qin, Q. (2015). *Determining the Low-Temperature Rheological Properties of Asphalt Binder Using a Dynamic Shear Rheometer (DSR)*. Laramie, WY 82072. Retrieved from Fundamental Properties of Asphalts and Modified Asphalts III Product: FP 08.

FHWA. (2017). *Four-mm Dynamic Shear Rheometry*. VA. Retrieved from TechBrief.

Ghavibazoo, A., & Abdelrahman, M. (2014). Effect of Crumb Rubber Dissolution on Low-Temperature Performance and Aging of Asphalt-Rubber Binder. *Transportation Research Record: Journal of the Transportation Research Board, 2445*, 47-55. doi: 10.3141/2445-06

Ghavibazoo, A., Abdelrahman, M., & Ragab, M. (2013). Mechanism of Crumb Rubber Modifier Dissolution into Asphalt Matrix and Its Effect on Final Physical Properties of Crumb Rubber-Modified Binder. *Transportation Research Record: Journal of the Transportation Research Board*(2370), 92-101. doi: 10.3141/2370-12

Hanz, A. J. (2012). *Quantifying the Impacts of Warm Mix Asphalt on Constructability and Performance.* (Doctor of Philosophy), University of Wisconsin – Madison, Wisconsin.

Hintz, C., & Bahia, H. (2013). Simplification of Linear Amplitude Sweep Test and Specification Parameter. *Transportation Research Record: Journal of the Transportation Research Board, 2370*, 10-16. doi: 10.3141/2370-02

Hintz, C., Velasquez, R., Johnson, C., & Bahia, H. (2011). Modification and Validation of Linear Amplitude Sweep Test for Binder Fatigue Specification. *Transportation Research Record: Journal of the Transportation Research Board, 2207*, 99-106. doi: 10.3141/2207-13

Huang, S. C. (2008). Rubber concentrations on rheology of aged asphalt binders. *Journal of Materials in Civil Engineering, 20*(3), 221-229. doi: 10.1061/(Asce)0899-1561(2008)20:3(221)

Lo Presti, D. (2013). Recycled Tyre Rubber Modified Bitumens for road asphalt mixtures: A literature review. *Construction and Building Materials, 49*, 863-881. doi: 10.1016/j.conbuildmat.2013.09.007

Malusky, J. J. (2016). *Evaluation of Laboratory Performance in MSCR Testing (T350/D7405) Using AMRL PSP Data*. Retrieved from http://www.asphaltetgs.org/

Marasteanu, M. O., & Cannone Falchetto, A. (2018). Review of experimental characterisation and modelling of asphalt binders at low temperature. *International Journal of Pavement Engineering, 19*(3), 279-291. doi: 10.1080/10298436.2017.1347436

Masad, E. A., Huang, C.-W., DAngelo, J., & Little, D. N. (2009). Characterization of asphalt binder resistance to permanent deformation based on nonlinear viscoelastic analysis of multiple stress creep recovery (MSCR) test. *Journal of the Association of Asphalt Paving Technologists, 78*

Maupin Jr., G. W. (1996). Hot mix asphalt rubber applications in Virginia. *Transportation Research Record: Journal of the Transportation Research Board*(1530), 18-24

Mikhailenko, P., Kadhim, H., & Baaj, H. (2017). Observation of bitumen microstructure oxidation and blending with ESEM. *Road Materials and Pavement Design, 18*(sup2), 216-225. doi: 10.1080/14680629.2017.1304251

National Asphalt Pavement Association. (2008). *Warm mix asphalt: Contractors' Experiences*. Lanham, Maryland.

Pasquini, E., Canestrari, F., Cardone, F., & Santagata, F. A. (2011). Performance evaluation of gap graded Asphalt Rubber mixtures. *Construction and Building Materials, 25*(4), 2014-2022. doi: 10.1016/j.conbuildmat.2010.11.048

Ragab, M., & Abdelrahman, M. (2014). Effects of Interaction Conditions on Internal Network Structure of Crumb Rubber-Modified Asphalts. *Transportation Research Record: Journal of the Transportation Research Board, 2444*, 130-141. doi: 10.3141/2444-15

Rubio, M. C., Martínez, G., Baena, L., & Moreno, F. (2012). Warm mix asphalt: an overview. *Journal of Cleaner Production, 24*, 76-84. doi: 10.1016/j.jclepro.2011.11.053

Rymer, B., & Donavan, P. (2005). Tire-pavement Noise Intensity Testing in Europe: The NITE Study and Its Relationship to Ongoing Caltrans Quiet Pavement Activities. *Journal of the Association of Asphalt Paving Technologists, 74*, 1107-1160

Safaei, F., & Castorena, C. (2016). Temperature Effects of Linear Amplitude Sweep Testing and Analysis. *Transportation Research Record: Journal of the Transportation Research Board, 2574*, 92-100. doi: 10.3141/2574-10

Shen, J., & Amirkhanian, S. (2007). The influence of crumb rubber modifier (CRM) microstructures on the high temperature properties of CRM binders. *International Journal of Pavement Engineering, 6*(4), 265-271. doi: 10.1080/10298430500373336

Shu, X., & Huang, B. S. (2014). Recycling of waste tire rubber in asphalt and portland cement concrete: An overview. *Construction and Building Materials, 67*, 217-224. doi: 10.1016/j.conbuildmat.2013.11.027

Stempihar, J., Gundla, A., & Underwood, B. S. (2018). Interpreting Stress Sensitivity in the Multiple Stress Creep and Recovery Test. *Journal of Materials in Civil Engineering, 30*(2). doi: 10.1061/(asce)mt.1943-5533.0002153

Sui, C., Farrar, M., Harnsberger, P., Tuminello, W., & Turner, T. (2011). New Low-Temperature Performance-Grading Method. *Transportation Research Record: Journal of the Transportation Research Board, 2207*, 43-48. doi: 10.3141/2207-06

Wang, H., Liu, X., Apostolidis, P., & Scarpas, T. (2018a). Non-Newtonian Behaviors of Crumb Rubber-Modified Bituminous Binders. *Applied Sciences, 8*(10), 1760. doi: 10.3390/app8101760

Wang, H., Liu, X., Apostolidis, P., & Scarpas, T. (2018b). Review of warm mix rubberized asphalt concrete: Towards a sustainable paving technology. *Journal of Cleaner Production, 177*, 302-314. doi: 10.1016/j.jclepro.2017.12.245

Wang, H., Liu, X., Apostolidis, P., & Scarpas, T. (2018c). Rheological Behavior and Its Chemical Interpretation of Crumb Rubber Modified Asphalt Containing Warm-Mix Additives. *Transportation Research Record: Journal of the Transportation Research Board*. doi: 10.1177/0361198118781376

Yu, B., Jiao, L., Ni, F., & Yang, J. (2014). Evaluation of plastic–rubber asphalt: Engineering property and environmental concern. *Construction and Building Materials, 71*, 416-424. doi: 10.1016/j.conbuildmat.2014.08.075

Yu, H., Leng, Z., Xiao, F., & Gao, Z. (2016). Rheological and chemical characteristics of rubberized binders with non-foaming warm mix additives. *Construction and Building Materials, 111*, 671-678. doi: 10.1016/j.conbuildmat.2016.02.066

Table 1. Basic properties of CRM.

Properties	**Description or value**
Source	Scrap truck tyres
Colour	Black
Morphology	Porous
Specific gravity (g/cm^3)	1.15
Decomposition temperature (°C)	~200
Total rubber (natural and synthetic)	55
Carbon Black (%)	30
Zinc oxide (%)	1.5
Sulphur (%)	1
Benzene extraction (%)	5.5
Ash content (%)	7

Table 2. MSCR Test Results of Different Asphalt Binders.

Binder type	J_{nr} **(1/kPa)**		J_{nrdiff} **(%)**	$J_{nrslope}$ **(%)**	**Percent recovery (%)**	
	0.1 kPa	**3.2 kPa**			**0.1 kPa**	**3.2 kPa**
70/100	7.604	8.431	10.9	26.7	2.03	0.85
70/100-W	2.573	5.373	108.8	90.3	28.38	2.35
70/100-C	8.020	8.751	9.1	23.6	4.48	1.64
CRMA	0.019	0.205	974.9	6.0	96.73	42.94
CRMA-W	0.019	0.262	1310.8	7.9	92.76	41.25
CRMA-C	0.158	0.741	370.3	18.8	79.61	26.99

Table 3. Analysis of LAS Results.

Sample code	***A***	***B***	C_1	C_2	N_f **(@2.5%)**	N_f **(@5.0%)**	**Failure energy (J)**
70/100	3.672×10^4	2.212	0.033	0.632	4,840	1,045	8,628
70/100-W	7.112×10^4	2.449	0.077	0.474	7,541	1,381	9,912
70/100-C	4.933×10^4	2.285	0.032	0.628	6,079	1,247	9,374
CRMA	2.171×10^7	3.539	0.127	0.334	848,332	73,006	28,585
CRMA-W	1.703×10^7	3.491	0.191	0.278	695,424	61,871	24,554
CRMA-C	6.553×10^6	3.160	0.223	0.354	362,181	40,517	17,776

Table 4. Analysis of shear relaxation modulus master curve.

Sample code	**Fitted equation**	$\mathbf{R^2}$	$G(60\ \mathbf{s})$ **(MPa)**	$m_r(60\ \mathbf{s})$
70/100	$y = -0.0649x^2 - 0.3893x + 7.9313$	0.9999	10.78	0.62
70/100-W	$y = -0.0540x^2 - 0.3471x + 7.9886$	1	15.84	0.54
70/100-C	$y = -0.0629x^2 - 0.4251x + 7.8029$	1	7.03	0.65
CRMA	$y = -0.0406x^2 - 0.3144x + 7.6338$	1	8.82	0.46
CRMA-W	$y = -0.0314x^2 - 0.3563x + 7.5926$	1	7.23	0.47
CRMA-C	$y = -0.0335x^2 - 0.4026x + 7.4168$	1	3.93	0.52

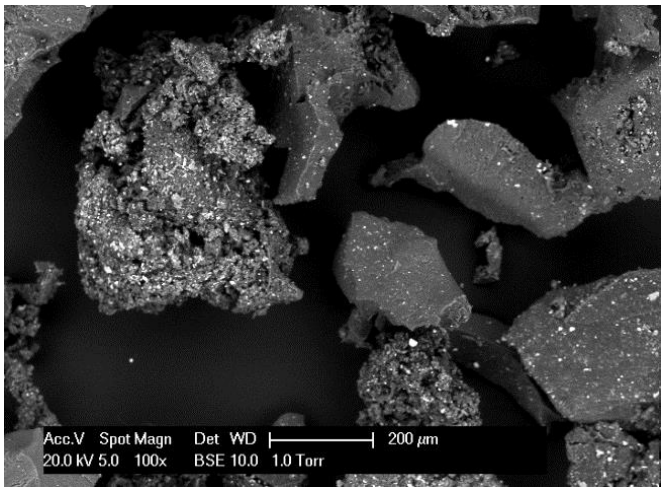

(a)

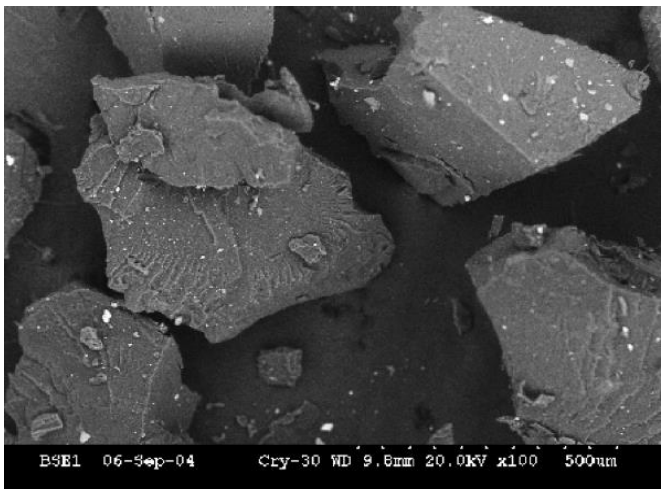

(b)

Figure 1. ESEM images of CRM processed by (a) ambient grinding (b) cryogenic grinding, adapted from (Shen & Amirkhanian, 2007).

(a) (b) (c)

Figure 2. ESEM sample preparation process (a) heat and casting (b) flattening and transferring (c) storing.

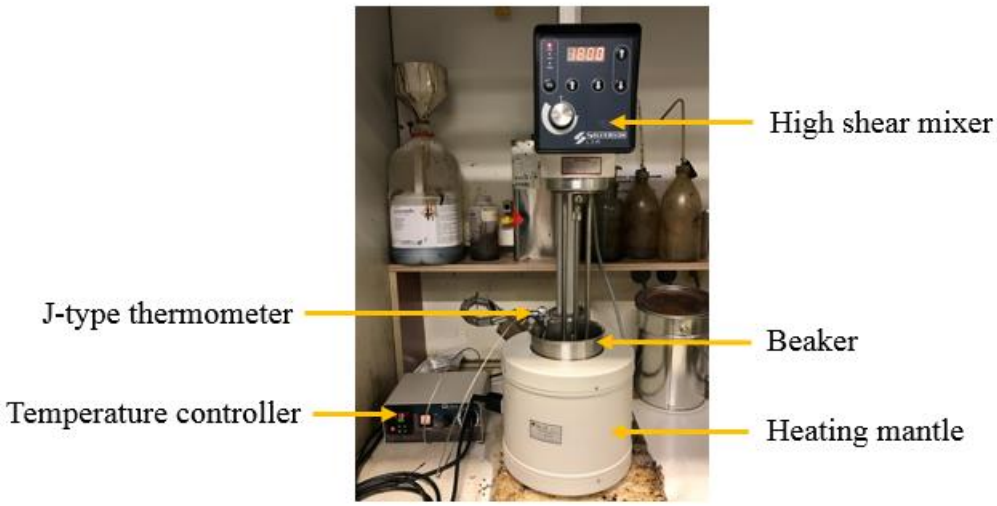

Figure 3. Laboratory equipment used to prepare CRMA binders.

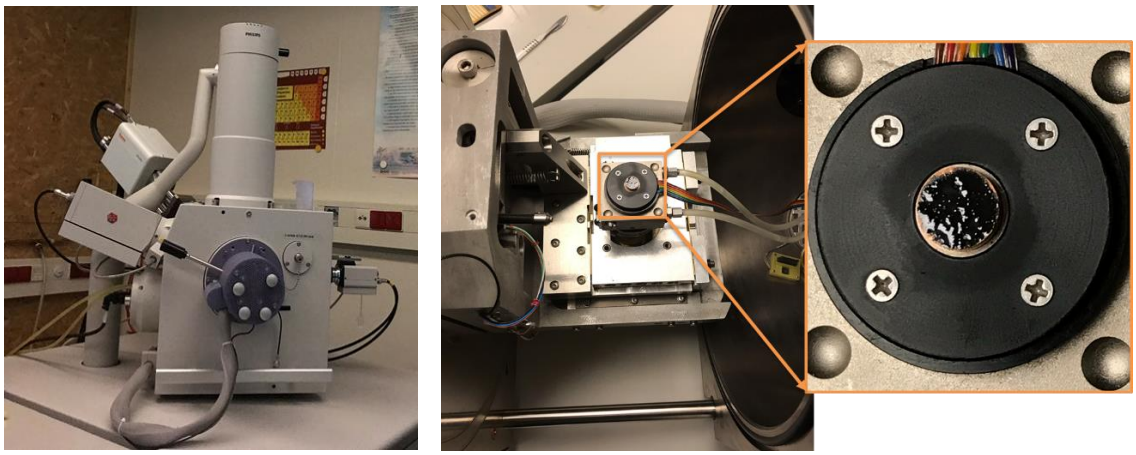

(a) (b)

Figure 4. ESEM apparatus (a)entirety (b) sample on the stage in the chamber.

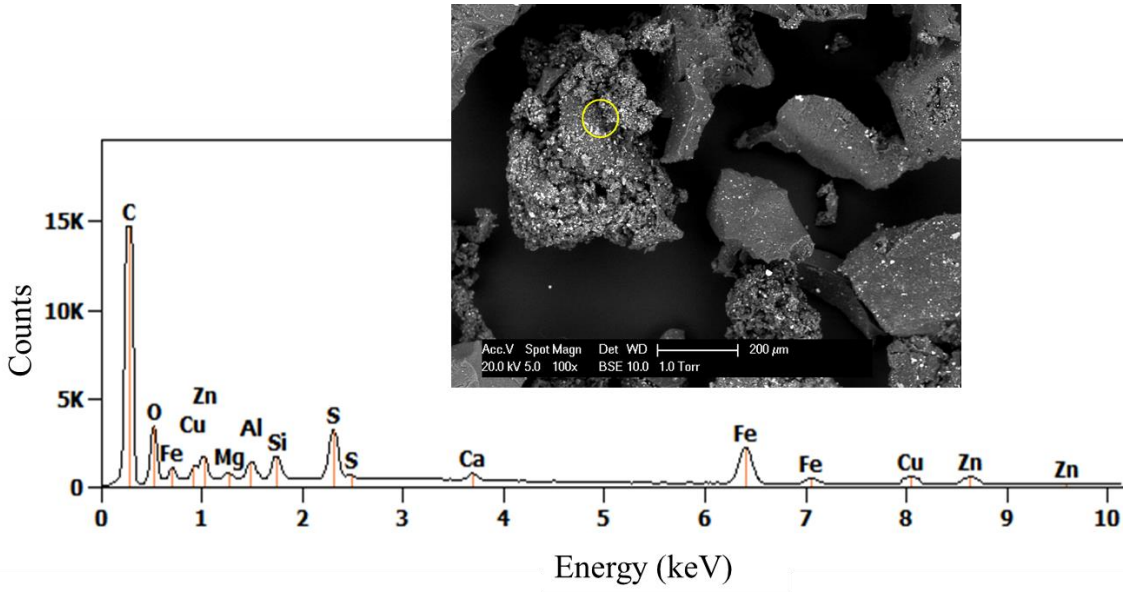

Figure 5. ESEM image and EDX spectrum of ambient CRM.

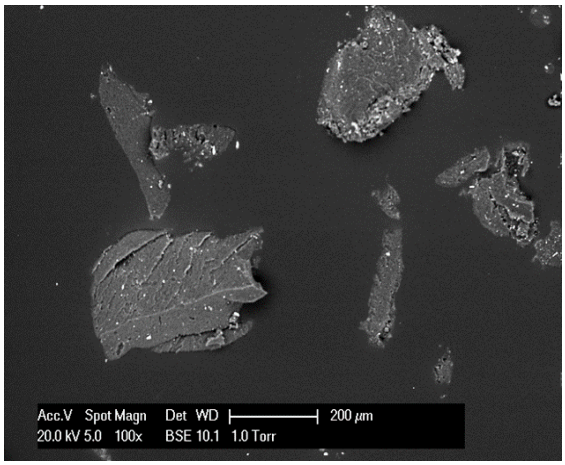

(a) reference state

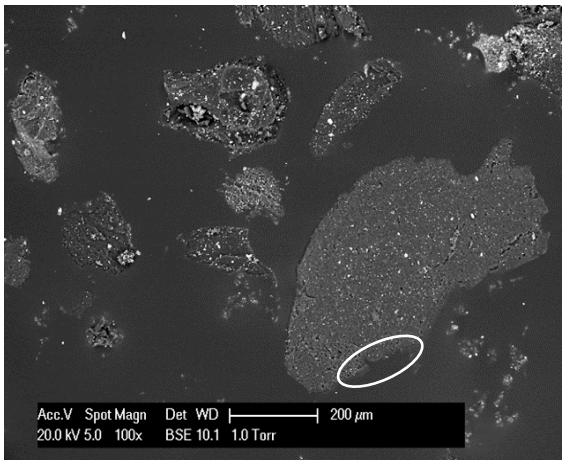

(b) 160 °C for 30 min

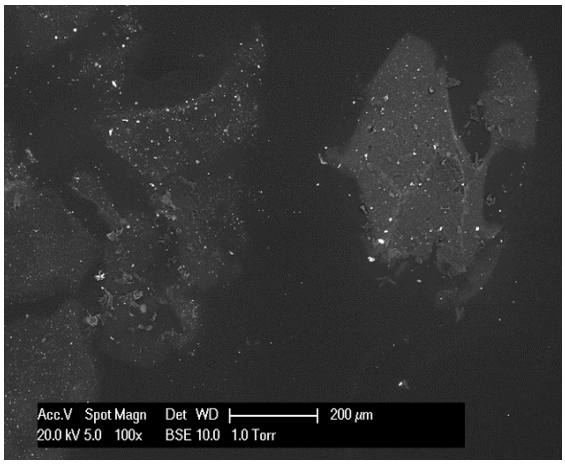

(c) 180 °C for 30 min

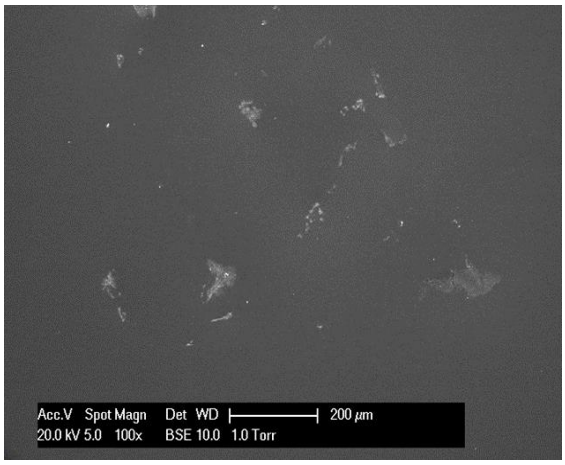

(d) 200 °C for 30 min

Figure 6. ESEM images for asphalt-rubber blend at different interaction conditions.

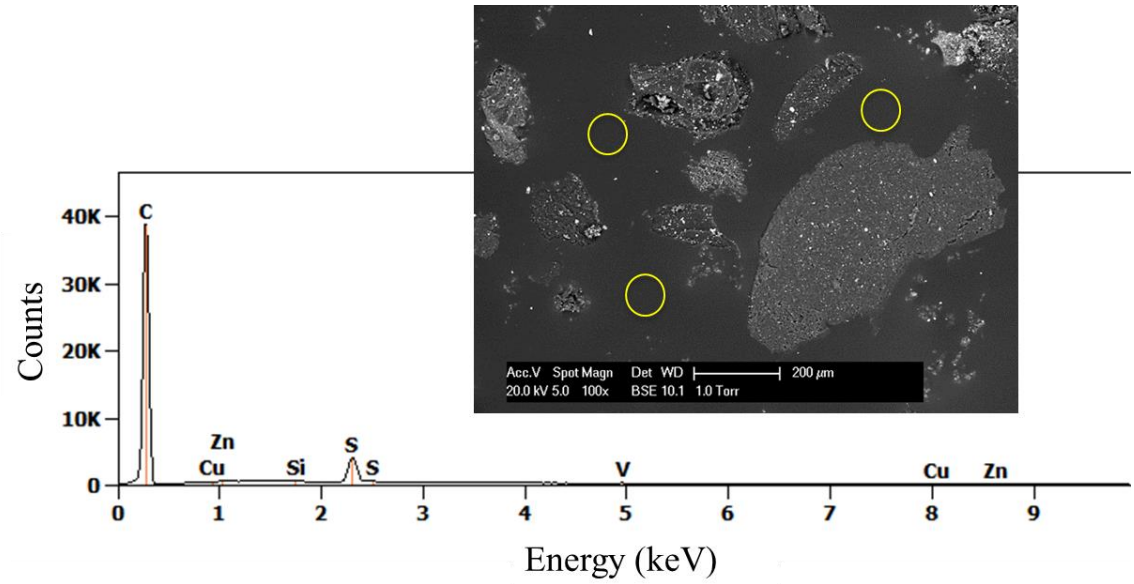

Figure 7. EDX spectrum of asphalt-rubber blend interacted at 160 °C.

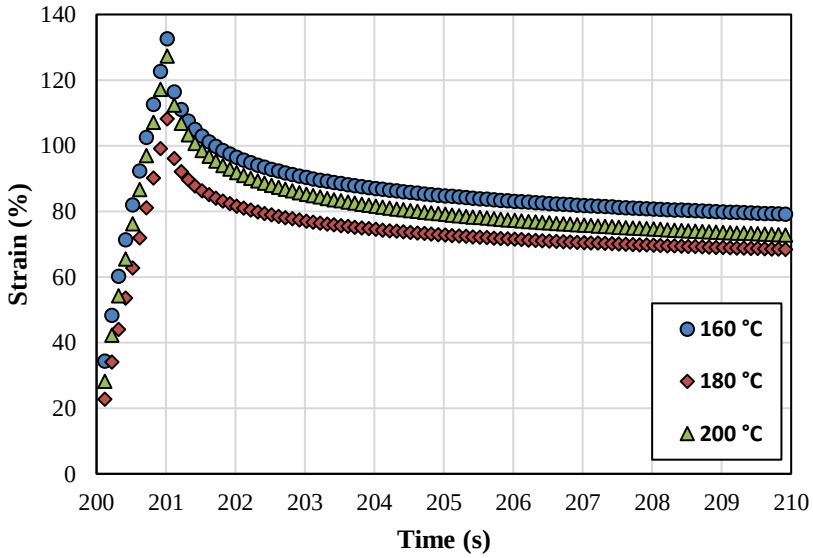

Figure 8. Creep and recovery cycle at 3.2 kPa for CRMA binders prepared at different temperatures.

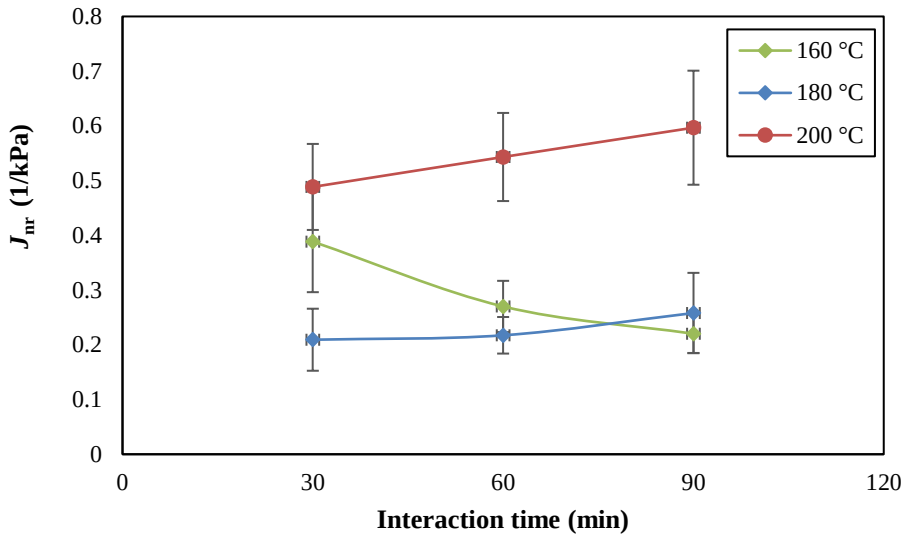

(a)

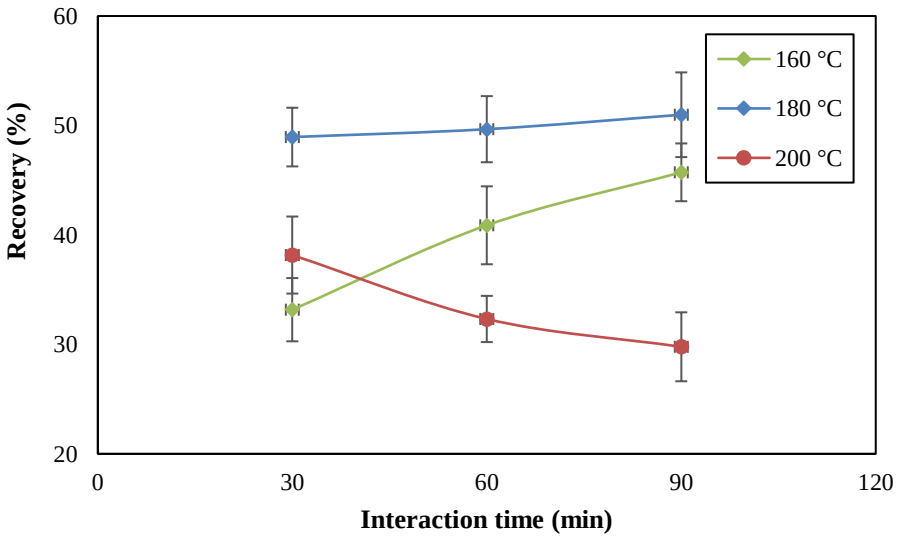

(b)

Figure 9. MSCR test results as a function of interaction temperature and time: (a) Nonrecoverable creep compliance and (b) percentage of recovery.

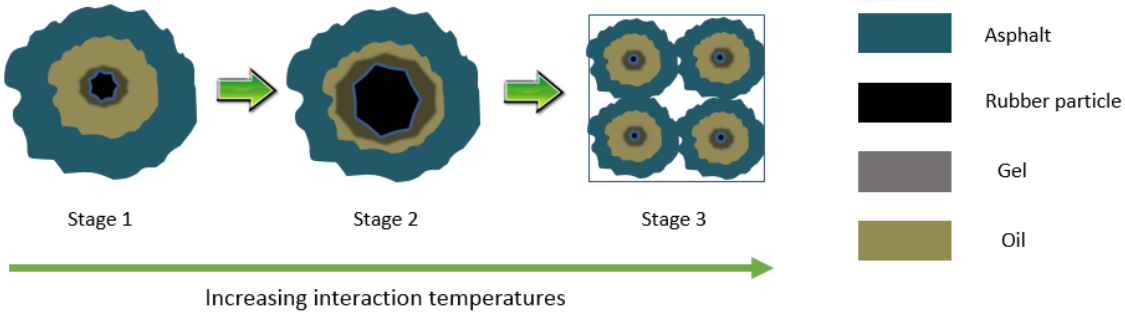

Figure 10. Schematic diagram of asphalt-rubber interaction stages.

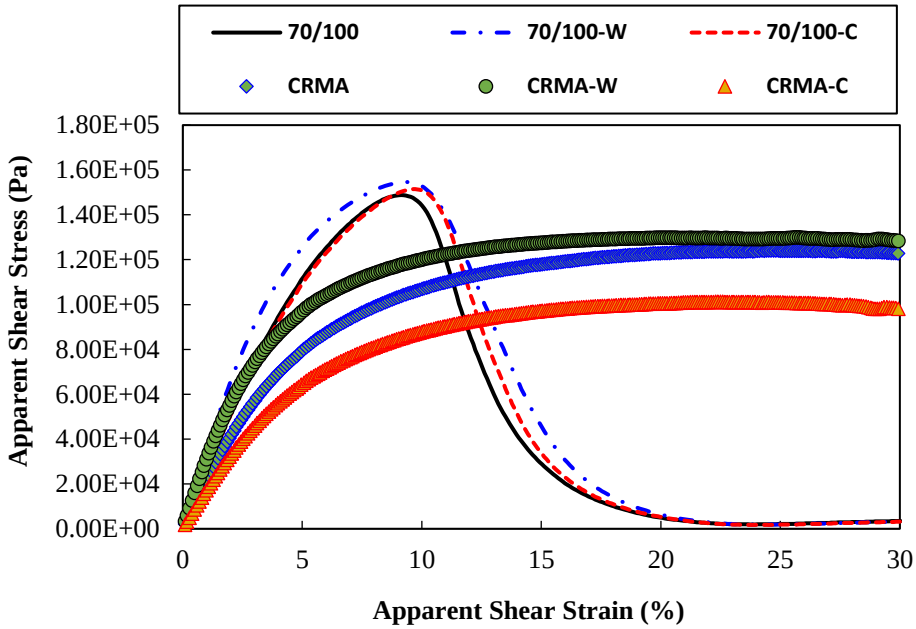

Figure 11. Shear stress and strain output from LAS test for different binders.

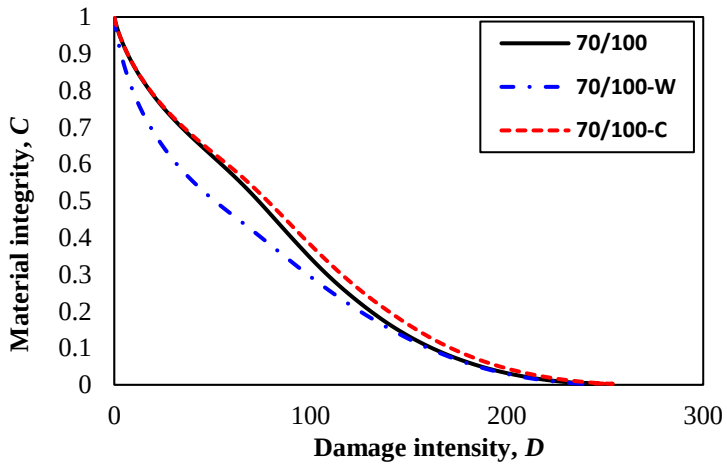
70/100
70/100-W
70/100-C
Material integrity, C
Damage intensity, D
0
0.1
0.2
0.3
0.4
0.5
0.6
0.7
0.8
0.9
1
0
100
200
300

(a)

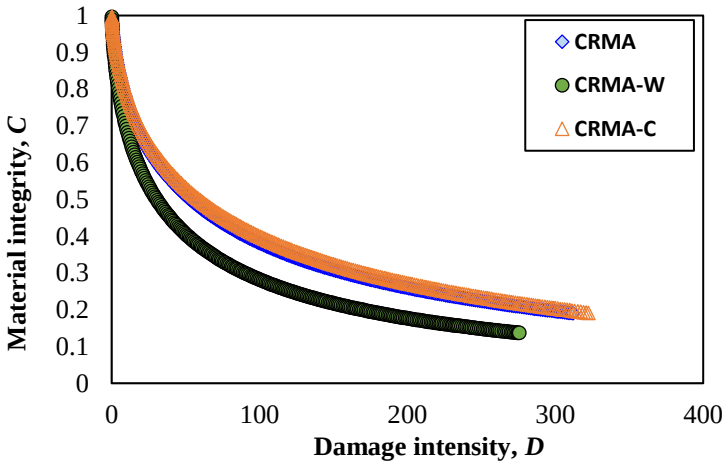
CRMA
CRMA-W
CRMA-C
Material integrity, C
Damage intensity, D
0
0.1
0.2
0.3
0.4
0.5
0.6
0.7
0.8
0.9
1
0
100
200
300
400

(b)

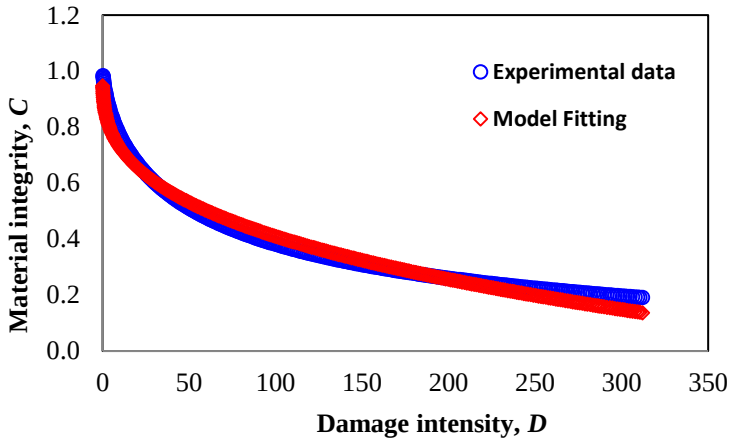
Experimental data
Model Fitting
Material integrity, C
Damage intensity, D
0.0
0.2
0.4
0.6
0.8
1.0
1.2
0
50
100
150
200
250
300
350

(c)

Figure 12. LAS material integrity versus damage intensity curves of (a) base asphalt with and without WMA additives, (b) CRMA binder with and without WMA additives, (c) comparison between experimental data and model fitting of CRMA binder.

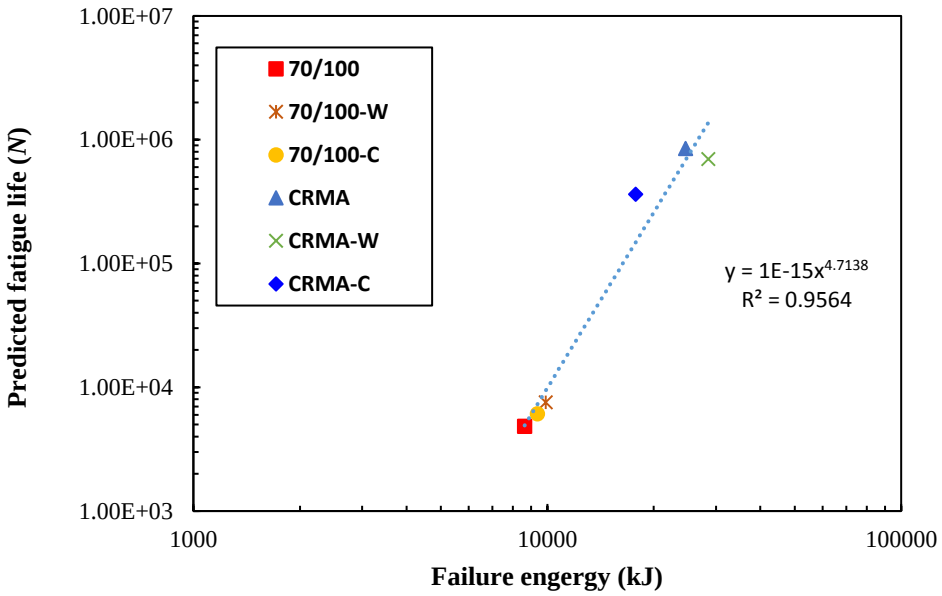

Figure 13. Correlation between predicted fatigue life and failure energy.

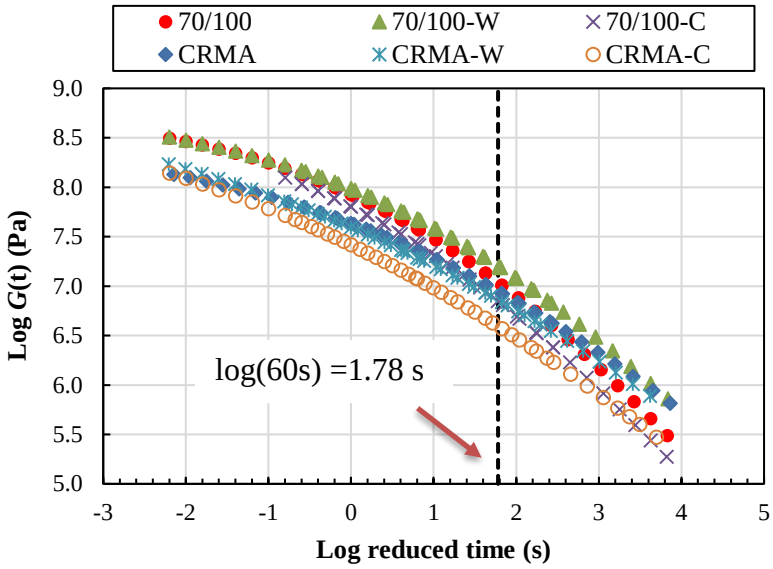

Figure 14. Master curve of shear stress relaxation modulus G(t) at a reference temperature of -10 °C.

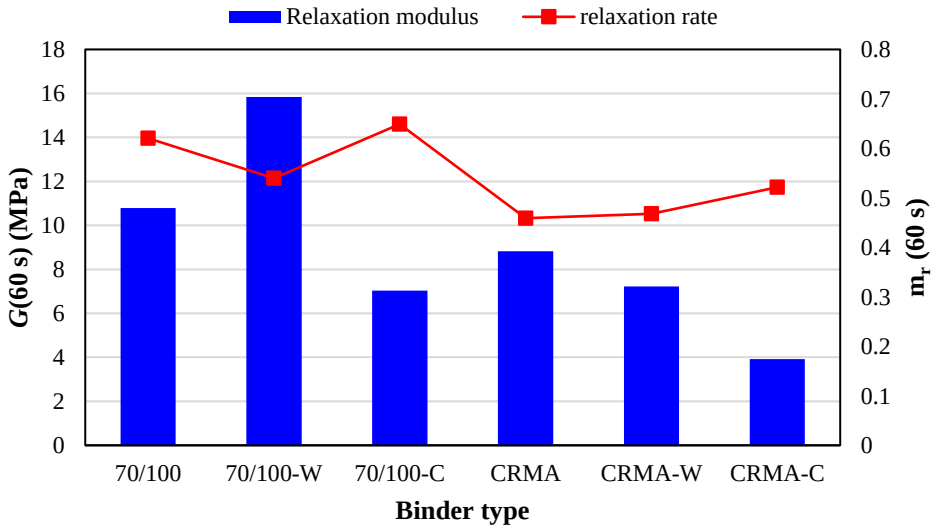

Figure 15. Derived $G(60\ s)$ and $m_r(60\ \mathrm{s})$ values of different binders at -10 °C.